Clock shifts in a Fermi gas interacting with a minority component: A soluble model

G. M. Bruun,[1,2] C. J. Pethick,[1,3] and Zhenhua Yu[3]
[1]*NORDITA, Roslagstullsbacken 23, SE-10691 Stockholm, Sweden*
[2]*Mathematical Physics, Lund Institute of Technology, P.O. Box 118, SE-22100 Lund, Sweden*
[3]*The Niels Bohr International Academy, The Niels Bohr Institute, Blegdamsvej 17, DK-2100 Copenhagen Ø, Denmark*
(Received 23 January 2010; published 23 March 2010)

We consider the absorption spectrum of a Fermi gas mixed with a minority species when majority fermions are transferred to another internal state by an external probe. In the limit when the minority species is much more massive than the majority one, we show that the minority species may be treated as static impurities and the problem can be solved in closed form. The analytical results bring out the importance of vertex corrections, which change qualitatively the nature of the absorption spectrum. It is demonstrated that large line shifts are not associated with resonant interactions in general. We also show that the commonly used ladder approximation fails when the majority component is degenerate for large mass ratios between the minority and majority species and that bubble diagrams, which correspond to the creation of many particle-hole pairs, must be taken into account. We carry out detailed numerical calculations, which confirm the analytical insights, and we point out the connection to shadowing phenomena in nuclear physics.

DOI: 10.1103/PhysRevA.81.033621 PACS number(s): 03.75.Ss, 05.30.Fk, 67.85.Jk

I. INTRODUCTION

The spectroscopy of spin excitations in atomic systems is important for basic science as well as being technologically relevant to atomic clocks. The subject has a long history, going back to studies of spin-exchange optical pumping [1] and of line shifts in hydrogen masers [2]. In recent years it has acquired renewed interest following experiments on ultracold atomic gases that have played an important role in probing effects of interatomic interactions in these systems [3–6]. In a typical experiment, one induces transitions of atoms from one hyperfine state of the ground-state manifold, denoted by 1, to a second hyperfine state, 2, in the presence of atoms in a third state, 3. Particular interest has focused on situations where the interatomic interactions are strong, for example, for ^{6}Li for which scattering lengths have magnitudes $\sim 10^3 a_0$ for a large range of magnetic fields.

The quantity measured in experiment is basically a two-particle correlation function that is difficult to calculate when interactions are strong. Many effects have to be considered, including particle self-energies, vertex corrections, pairing, and the inhomogeneity of the atomic cloud [7–16]. In this article we consider a simple model where the mass of the bystander atom, 3, is much larger that of states 1 and 2. This allows us to include self-energy and vertex corrections to all orders in a conserving approximation which becomes exact when the system is highly polarized, in the sense that the density of the bystander atoms is much smaller than the density of the 1 atoms. For brevity, we shall refer to an atom in state i ($i = 1, 2, 3$) as an i-atom. Throughout most of the article we shall neglect the interaction between 1- and 2-atoms which does not give rise to shifts in the absence of interactions with 3-atoms. For densities of 3-atoms low enough that they are nondegenerate, the statistics of these atoms plays no role, so our calculations apply to both bosons and fermions.

Our formalism enables us to derive analytic results, and for the case of nondegenerate majority atoms these agree with ones obtained previously [1,2]. The calculations bring out the important role of the processes analogous to those considered by Aslamazov and Larkin [17] in studies of fluctuation contributions to response functions close to the transition temperature in superconducting metals.

We find that vertex corrections can qualitatively change the clock shift compared with the prediction without vertex corrections. We also show that large line shifts are not associated with resonant interactions. For instance, when one interaction, e.g., 1-3, is on resonance, the clock shift has the same magnitude *but the opposite sign* compared with its value when the 1-3 interaction is zero. Our analytical results are confirmed by numerical calculations. Another conclusion of the work is that for the case of massive bystander atoms, the common approximation of including only ladder diagrams is inadequate, since particle-hole correlations must be considered on the same footing at particle-particle and hole-hole correlations. We also discuss the relationship of the physics of the clock shift problem to the phenomenon of "shadowing" in nuclear physics, the fact that, e.g., the total cross section for scattering of a pion from the deuteron is not equal to the sum of the cross section for scattering from a proton and that for scattering from a neutron [18].

This article is organized as follows. In Sec. II we describe the basic formalism for calculating the transition rate, and in Sec. III we describe the calculation of the line shape under the assumption that the massive atoms may be treated as static impurities. After deriving analytical result we present results of numerical calculations. Section IV is devoted to showing from diagrammatic perturbation theory that for a mobile minority species with a large mass, the problem reduces to that of scattering from static impurities. There we also consider the relationship of our calculations to the x-ray edge problem and the phenomenon of "shadowing" in nuclear physics. Finally, Sec.V contains concluding remarks.

II. TRANSITION RATE

We consider a gas of fermions in an internal state 1 with density n_1 and mass m which interacts with a gas of fermions or bosons of mass m_3 and density n_3 which is assumed to be

much smaller than n_1. The gas is subjected to a homogeneous probe that flips the fermions from state 1 to state 2 at a rate which within linear response theory is proportional to

$$\sum_{i,f}(P_i - P_f)\left|\int d^3r\langle f|\psi_2^\dagger(\mathbf{r})\psi_1(\mathbf{r})|i\rangle\right|^2\delta(\omega - E_f + E_i), \tag{1}$$

where initial states are denoted by i and final ones by f and their energies by E_i and E_f. The frequency of the applied field is ω. (We put $\hbar$ and the Boltzmann constant equal to unity throughout.) The probability of occupation of the initial (final) state is denoted by P_i (P_f). The operator $\psi_\sigma^\dagger(\mathbf{r})$ creates a fermion in state σ at position $\mathbf{r}$. In terms of correlation functions, the rate is proportional to

$$\mathrm{Im}\mathcal{D}(\omega) \propto \int d\mathbf{r}d\mathbf{r}'\mathrm{Im}\mathcal{D}(\mathbf{r},\mathbf{r}',\omega), \tag{2}$$

where $\mathcal{D}(\mathbf{r},\mathbf{r}',\omega)$ is the Fourier transform of the quantity $-i\theta(t-t')\langle[\psi_2^\dagger(\mathbf{r},t)\psi_1(\mathbf{r},t),\psi_1^\dagger(\mathbf{r}',t')\psi_2(\mathbf{r}',t')]\rangle$ which may be regarded as the correlation function for the pseudospin operator that describes atoms in the states 1 and 2.

III. STATIC IMPURITIES

In this section, we consider the case when $m_3 \gg m$ so that the 3-atoms may be treated as static impurities, as we shall demonstrate in Sec. IV. We shall work at nonzero temperature T, in which case the frequencies are to be regarded initially as Matsubara frequencies, odd multiples of πT for fermions and even multiples for bosons. The real-time correlation function is then obtained in the standard way by analytically continuing from the imaginary time domain. The fermion propagators in the presence of the impurities are

$$G_\sigma(p,z)^{-1} = G_\sigma^0(p,z)^{-1} - \Sigma_\sigma(z), \tag{3}$$

where

$$G_\sigma^0(p,z)^{-1} = z - p^2/2m - \epsilon_\sigma + \mu_\sigma \tag{4}$$

is the bare propagator and $\Sigma_\sigma(z)$ the self-energy. Here ϵ_σ is the energy of a noninteracting σ-fermion ($\sigma = 1, 2$) at rest and μ_σ the chemical potential. In Eq. (3) it is understood that the propagator is averaged over a random distribution of impurities [19], but we shall not indicate this explicitly in the notation. A similar remark applies to the correlation function $\mathcal{D}(\omega)$.

To lowest order in n_3, the self-energy has the form

$$\Sigma_\sigma(z) = n_3\mathcal{T}_\sigma(z). \tag{5}$$

Here $\mathcal{T}_\sigma(z)$ is the T matrix for scattering of a σ-fermion on an impurity, which is given in a matrix notation by

$$\mathcal{T}_\sigma(z) = V_\sigma + V_\sigma G_\sigma(z)\mathcal{T}_\sigma(z), \tag{6}$$

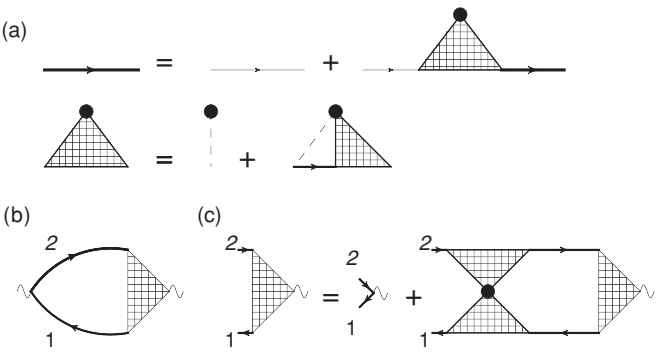

FIG. 1. (a) The propagator G for the fermions scattering on impurities. (b) The correlation function $\mathcal{D}(\omega)$. (c) The vertex function. Thick solid lines indicate G, thin solid lines G_0, and dashed lines scattering on a impurity marked by •.

where the momentum sums are implicit. We have assumed that the range of the interaction V_σ between the impurities and the fermions is much shorter than the lesser of the typical interparticle distance and the thermal de Broglie wavelength, $(2\pi/mT)^{1/2}$. In this case, for the momenta of interest, the scattering amplitude depends only on the energy. Equations (3)–(5) are shown diagrammatically in Fig. 1(a).

The correlation function $\mathcal{D}(\omega)$ is shown diagrammatically in Fig. 1(b) and the vertex function in Fig. 1(c). The importance of vertex corrections may be illustrated by considering the case when the interaction between an impurity and a fermion is the same for the two fermion species. The Hamiltonian is then SU(2) symmetric with respect to rotations between the states 1 and 2 and the correlation function $\mathcal{D}(\omega)$ is unaffected by interactions [8]. However, the self-energy corrections to the single-particle propagator are nonzero and they must therefore be canceled by the vertex corrections. To recover the SU(2) invariance and to satisfy conservation laws, it is necessary when calculating the correlation function to use as the vertex in the particle-hole channel the quantity $\delta\Sigma/\delta G$ (Σ and G are two-dimensional matrices in the Hilbert space spanned by the states 1 and 2) [8,20]. The structure of the vertex corrections is shown in Fig. 1(c). We now perform such a conserving calculation of $\mathcal{D}(\omega)$ which takes the effects of the impurities into account exactly to lowest order in n_3.

The vertex corrections correspond to processes in which a 2-particle and a 1-hole scatter from the same impurity. The resulting effective interaction [the "bow-tie" part of the diagram in Fig. 1(c)] is given by

$$V_{\mathrm{eff}} = n_3\mathcal{T}_1(i\omega_\nu)\mathcal{T}_2(i\omega_\nu + i\omega_\gamma), \tag{7}$$

since for a static impurity the energy transfer between particles and the impurity is zero. Because the scattering on an impurity is independent of momentum, the inclusion of the vertex corrections simplifies significantly, and the diagrams for the correlation function may be summed. The result is

$$\mathcal{D}(i\omega_\gamma) = T\sum_{\omega_\nu}\frac{(2\pi)^{-3}\int d^3pG_1(p,i\omega_\nu)G_2(p,i\omega_\nu + i\omega_\gamma)}{1 - n_3\mathcal{T}_1(i\omega_\nu)\mathcal{T}_2(i\omega_\nu + i\omega_\gamma)(2\pi)^{-3}\int d^3pG_1(p,i\omega_\nu)G_2(p,i\omega_\nu + i\omega_\gamma)} \tag{8}$$

with ω_ν being a fermion Matsubara frequency and ω_γ a boson one. The momentum integral yields

$$M(z_1, z_2) = \int \frac{d^3p}{(2\pi)^3} G_1(p, z_1) G_2(p, z_2) = i\pi \frac{d_2(z_2)\mathrm{sgn}(\mathrm{Im}z_2) - d_1(z_1)\mathrm{sgn}(\mathrm{Im}z_1)}{z_2 - z_1 + \mu_2 - \mu_1 - \Delta + \Sigma_1(z_1) - \Sigma_2(z_2)} \tag{9}$$

with $d_\sigma(z) = m^{3/2}\sqrt{z + \mu_\sigma - \epsilon_\sigma - \Sigma_\sigma(z)}/\sqrt{2}\pi^2$ and $\Delta = \epsilon_2 - \epsilon_1$ the hyperfine splitting between the two fermionic states. For $\Sigma = 0$, d is the free particle density of states. We evaluate the sum over Matsubara frequencies in (8) by converting it to a contour integration in the usual way by multiplying the integrand by the Fermi function $f(z_1) = [\exp(\beta z_1) + 1]^{-1}$ and choosing a contour that encircles the poles of the Fermi function. The integration contour may be deformed to lie above and below the cuts of the functions d_1 and d_2, which are located at $z_1 = \epsilon$ and $z_1 = \epsilon - i\omega_\gamma$, respectively, where ϵ is real. After the analytic continuation $i\omega_\gamma \to \tilde{\omega} + i\eta$, with the physical frequency given by $\omega = \tilde{\omega} + \mu_2 - \mu_1$, we obtain

$$\mathcal{D}(\omega) = -\int_{-\infty}^{\infty} \frac{d\epsilon}{2\pi i} f(\epsilon) [\mathcal{S}(\epsilon + i\eta, \epsilon + \tilde{\omega} + i\eta) - \mathcal{S}(\epsilon - i\eta, \epsilon + \tilde{\omega} + i\eta) + \mathcal{S}(\epsilon - \tilde{\omega} - i\eta, \epsilon + i\eta) - \mathcal{S}(\epsilon - \tilde{\omega} - i\eta, \epsilon - i\eta)], \tag{10}$$

where

$$\mathcal{S}(z_1, z_2) = \frac{M(z_1, z_2)}{1 - n_3 \mathcal{T}_1(z_1)\mathcal{T}_2(z_2) M(z_1, z_2)}. \tag{11}$$

The imaginary part of the correlation function becomes

$$\mathrm{Im}\mathcal{D}(\omega) = \int \frac{d\epsilon}{2}(f_2 - f_1)\mathrm{Im}\left[\frac{d_2 - d_1}{\omega - \Delta + n_3[\mathcal{T}_1 - \mathcal{T}_2 - i\pi\mathcal{T}_1\mathcal{T}_2(d_2 - d_1)]} - \frac{d_2 + d_1^*}{\omega - \Delta + n_3[\mathcal{T}_1^* - \mathcal{T}_2 - i\pi\mathcal{T}_1^*\mathcal{T}_2(d_2 + d_1^*)]}\right]. \tag{12}$$

In (12), $f_1 = f(\epsilon)$, $f_2 = f(\epsilon + \tilde{\omega})$, and d_1 and $\mathcal{T}_1$ are evaluated at the energy $\epsilon + i\eta$ and d_2 and $\mathcal{T}_2$ at the energy $\epsilon + \tilde{\omega} + i\eta$. The T matrix, given by Eq. (6), has the form

$$\mathcal{T}_\sigma = \frac{\mathcal{T}_{\sigma\,\mathrm{vac}}}{1 + i\pi d_\sigma \mathcal{T}_{\sigma\,\mathrm{vac}}}, \tag{13}$$

where $\mathcal{T}_{\sigma\,\mathrm{vac}}$ is the T matrix for σ fermions scattering at zero energy in a vacuum. From this it follows that Eq. (12) reproduces the unshifted ideal gas result when the interaction is SU(2) symmetric with identical scattering between an impurity and the two fermionic species. Note that it is crucial to use full propagators to recover this symmetry.

A. A simple limit

Equation (12) satisfies the conservation laws regardless of the magnitude of n_3. We now study the interaction effects on $\mathcal{D}(\omega)$ to the lowest order in n_3 and neglect all medium effects except the factor n_3 in front of the T matrices in the denominator in (12). The T matrix is thus replaced by its value in a vacuum given by

$$\mathcal{T}_\sigma = i\frac{e^{2i\delta_\sigma} - 1}{2\pi d_0}, \tag{14}$$

where δ_σ is the scattering phase shift in a vacuum and $d_0 = m^{3/2}\sqrt{\epsilon}/\sqrt{2}\pi^2$ is the free-particle density of states. For low energies, the phase shift is given in terms of the scattering length a_σ by $\tan\delta_\sigma = -ka_\sigma$, where $k = \sqrt{2m\epsilon}$.

We make the variable change $\epsilon + \mu_1 - \epsilon_1 \to \epsilon$, so that ϵ is the kinetic energy of a 1-fermion. The 2-fermion has kinetic energy $\epsilon + \omega - \Delta$. In the limit of a low density of 3-atoms, the line shifts are small. One may then neglect differences between ω and Δ, and therefore the phase shifts of the two fermions are to be evaluated at the same kinetic energy. In total, keeping only the lowest order effects of n_3 in (12) yields

$$\mathrm{Im}\mathcal{D}(\omega) \simeq \mathrm{Im}\int_0^\infty d\epsilon \frac{-d_0 f(\epsilon + \epsilon_1 - \mu_1)}{\omega - \Delta - in_3[e^{2i(\delta_1 - \delta_2)} - 1]/2\pi d_0}. \tag{15}$$

We have written Eq. (15) for the case where there are no 2-fermions present initially so that the first Fermi function in Eq. (12) is zero. This corresponds to a typical experimental situation. For equal interaction between the impurity and the initial 1- and final 2-fermions, i.e., for $\delta_1 = \delta_2$, one sees immediately that the interaction effects vanish in the denominator of (15) and we recover the ideal gas result

$$\mathcal{D}(\omega) = -\frac{n_1}{\omega - \Delta + i\eta}. \tag{16}$$

In general, $\mathrm{Im}\mathcal{D}(\omega)$ is the sum of Lorentzian lines, with the energy-dependent frequency shift

$$\Delta\omega(\epsilon) = n_3\frac{\pi}{m}\frac{\sin(2\delta_1 - 2\delta_2)}{k}, \tag{17}$$

and with full width at half maximum equal to

$$\Gamma(\epsilon) = n_3\frac{4\pi}{m}\frac{\sin^2(\delta_1 - \delta_2)}{k}. \tag{18}$$

Equations (17) and (18), which apply for arbitrary degree of degeneracy of the 1-atoms, have a form similar to those derived for a classical gas in Refs. [1], Eq. (82) and [2], which studied the equation of motion for the density matrix. There is, however, a difference, since to obtain the result in these articles one must replace the term containing the phase shifts in the denominator of Eq. (15) by its thermal average. Since Δ and Γ are energy dependent, the line shape given by Eq. (15) will

not be Lorentzian in general. The magnitude of deviations from Lorentzian behavior will depend on the variation of $[e^{2i(\delta_1-\delta_2)}-1]/k$, over the distribution of the momentum k of 1-atoms.

For small phase shifts, $\delta_\sigma \simeq k a_\sigma$ and Eq. (17) reproduces the low-density expression for the shift, $\Delta\omega \simeq n_3 2\pi(a_2 - a_1)/m$, the factor of 2, rather than the usual factor of 4 for the case of fermions of equal mass, being due to the fact that we have taken the 3-atoms to be infinitely massive.

Equations (17) and (18) clearly illustrate the importance of vertex corrections. When these are neglected, the corresponding results are

$$\Delta\omega(\epsilon)|_{\text{no vertex}} = n_3 \frac{\pi}{m} \frac{\sin 2\delta_1 - \sin 2\delta_2}{k}, \tag{19}$$

and

$$\Gamma(\epsilon)|_{\text{no vertex}} = n_3 \frac{4\pi}{m} \frac{\sin^2\delta_1 + \sin^2\delta_2}{k}. \tag{20}$$

There are a number of important conclusions that may be drawn from the above results. First, without vertex corrections the shift and damping do not display the required SU(2) symmetry for $\delta_1 = \delta_2$. Second, for small phase shifts the line width is proportional to $(a_1 - a_2)^2$, whereas without vertex corrections the corresponding result is $a_1^2 + a_2^2$. Thus, even in the limit of small phase shifts it is important to include vertex corrections, which give an interference term $-2a_1a_2$. Third, the largest shifts are obtained for $\delta_1 - \delta_2 \approx \pi/4 + \nu\pi/2$, where ν is an integer. Thus, resonant scattering is not particularly favorable for producing large shifts. For example, take a typical experimental situation where scattering of the fermions in the initial state 1 with 3-atoms is resonant while that of final state 2 fermions is not: the shift is then equal in magnitude but *of the opposite sign* compared with what it would be in the absence of 1-3 scattering, and therefore the magnitude of the shift is determined completely by the nonresonant 2-3 interaction. Finally, large widths and large shifts do not go hand in hand, since the largest widths occur when $\delta_1 - \delta_2$ is an odd multiple of $\pi/2$.

B. Numerical results

In Figs. 2 and 3 we present numerical results for $\mathrm{Im}\mathcal{D}(\omega)$ obtained from Eq. (12). The propagators used in this calculation are determined fully self-consistently. The frequency unit is $\pi n_3/mk_F$ with $n_1 = k_F^3/6\pi^2$ [see (17) and (18)], and $\mathrm{Im}\mathcal{D}(\omega)$ plotted in units of mk_F. In Fig. 2, we show the transition rate for $T = 0$ and with an impurity density $n_3/n_1 = 0.1$. The scattering length for the 2-3 interaction is $a_2 = -1/k_F$ and the scattering length for the 1-3 interaction varies from $a_1 = 0$ to $a_1 = -100/k_F$, which is very close to resonance. For $k_F a_1 = 0$, the line shift and width are due solely to the self-energy of the 2-atom. We see that when the 1-3 interaction is resonant, the main effect is to change the sign of line shift compared with the result for zero 1-3 interaction. This confirms the discussion in subsection III A. When $k_F a_1 = k_F a_2 = -1$, the unshifted ideal gas result is recovered, as it should be, and the small remaining width of the calculated signal is entirely due to a small imaginary part we have added explicitly to the frequency to facilitate the numerical calculations. For comparison, we also plot the result obtained for $k_F a_1 = k_F a_2 = -1$ when

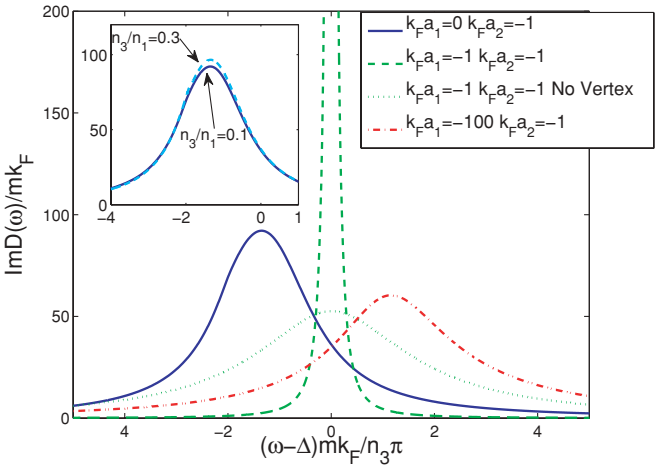

FIG. 2. (Color online) The transition rate as a function of frequency and interaction. The inset shows the transition rate for varying impurity concentration.

vertex corrections are not included. We see that, although the predicted line shift is small, the width is large and one does not recover the unshifted narrow line when vertex corrections are ignored.

In the inset, we compare the line shape for $n_3/n_1 = 0.1$ and $n_3/n_1 = 0.3$, keeping $k_F a_1 = 0$ and $k_F a_2 = -1$ fixed. To ease comparison of the results for the two different impurity concentrations, we have multiplied $\mathrm{Im}\mathcal{D}(\omega)$ by n_3. The two curves largely overlap which illustrates that the line shift and width essentially scale with n_3 in agreement with (17) and (18). Note that higher-order medium effects coming from the self-consistent determination of the propagators give rise to the slight difference between the results for the two impurity concentrations.

In Fig. 3, we plot the transition rate as a function of a_1 keeping $a_2 = 0$. The line shift is large, whereas the width is small for $k_F a_1 = -1$. This is in agreement with the conclusions reached in subsection III A from (17) and (18) since $k_F a_1 = -1$ corresponds to a phase shift of $\delta_1 = \pi/4$.

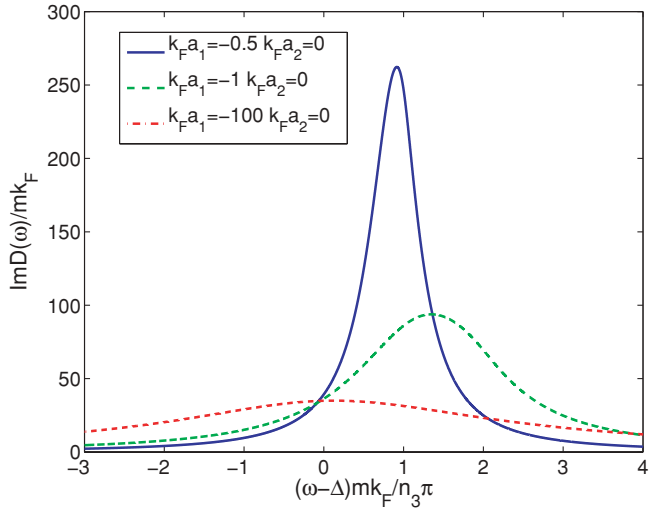

FIG. 3. (Color online) The transition rate as a function of frequency for varying initial state interaction.

Likewise, when the scattering is close to resonance with $k_F a_1 = -100$ corresponding to $\delta_1 \approx \pi/2$, the line shift is small, whereas the width is large. Again, this agrees with the discussion in subsection III A.

IV. MOBILE, MASSIVE IMPURITIES

In this section we show that in the limit $m/m_3 \to 0$, the results we have employed in Sec. III for the self-energy and vertex corrections may be derived from diagrammatic many-body theory for particles of finite mass. An important conclusion of this section is that the ladder approximation, which is commonly employed in treating strongly interacting systems is inadequate to describe systems with $m_3 \gg m$ when the 1-fermions are degenerate. We begin by showing this for low-order contributions in perturbation theory and then generalize the considerations to arbitrary order. For definiteness, we shall assume that the 3-atoms are fermions, but the calculations may easily be generalized to the case of bosons, the only difference being that the distribution function for 3-atoms must be taken to be the Bose distribution. To lowest order in the density of 3-atoms, the results are independent of the statistics of the 3-atoms.

A. Second order

In the Hartree approximation the self-energy and vertex corrections are given by Eqs. (5) and (7) when the T matrix is evaluated in the Born approximation, so the first term we shall consider in detail is the second-order term, Fig. 4(a). For $m/m_3 \to 0$ it is given by

$$\Sigma_1^{(2)}(p,\omega) = \int \frac{d^3q}{(2\pi)^3}\frac{d^3p'}{(2\pi)^3}|V_1(q)|^2 \times \frac{f^3_{\mathbf{p}'}\left(1-f^3_{\mathbf{p}'+\mathbf{q}}\right)\left(1-f^1_{\mathbf{p}-\mathbf{q}}\right)+\left(1-f^3_{\mathbf{p}'}\right)f^3_{\mathbf{p}'+\mathbf{q}}f^1_{\mathbf{p}-\mathbf{q}}}{\omega-(\mathbf{p}-\mathbf{q})^2/2m}, \tag{21}$$

where $V_\sigma(\mathbf{q})$ is the bare interaction between a 3-atom and a σ-fermion and $f^i_{\mathbf{p}} = f(p^2/2m_i + \epsilon_i - \mu_i)$. When the 3-atoms

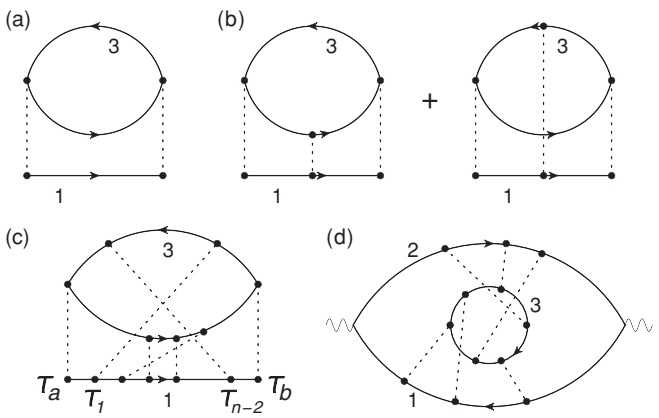

FIG. 4. Diagrams for the self-energy of a 1-fermion. (a) Second-order contributions. (b) Third-order contributions. (c) A general term. (d) A diagram with a general vertex correction. Solid lines are fermion propagators, dashed lines interactions with • indicating the vertices.

are nondegenerate the $1 - f^3$ factors may be replaced by unity, and one then finds

$$\Sigma_1^{(2)} = \int \frac{d^3q}{(2\pi)^3}\frac{d^3p'}{(2\pi)^3}|V_1(q)|^2\frac{f^3_{\mathbf{p}'}\left(1-f^1_{\mathbf{p}-\mathbf{q}}\right)+f^3_{\mathbf{p}'+\mathbf{q}}f^1_{\mathbf{p}-\mathbf{q}}}{\omega-(\mathbf{p}-\mathbf{q})^2/2m} = n_3\int\frac{d^3q}{(2\pi)^3}|V_1(q)|^2\frac{\left(1-f^1_{\mathbf{p}-\mathbf{q}}\right)+f^1_{\mathbf{p}-\mathbf{q}}}{\omega-(\mathbf{p}-\mathbf{q})^2/2m} = n_3\mathcal{T}^{(2)}_{\rm vac}, \tag{22}$$

where

$$\mathcal{T}^{(2)}_{\rm vac}(p,\omega) = \mathcal{T}^{(2)}_{\rm lad}(p,\omega)+\mathcal{T}^{(2)}_{\rm bub}(p,\omega) = \int\frac{d^3q}{(2\pi)^3}|V_1(q)|^2\frac{1}{\omega-(\mathbf{p}-\mathbf{q})^2/(2m)} \tag{23}$$

is the T matrix in a vacuum (calculated to second order in V_1). Here

$$\mathcal{T}^{(2)}_{\rm lad}(p,\omega) = \int\frac{d^3q}{(2\pi)^3}|V_1(q)|^2\frac{1-f^1_{\mathbf{p}-\mathbf{q}}}{\omega-(\mathbf{p}-\mathbf{q})^2/(2m)} \tag{24}$$

is the contribution to the T matrix from ladder diagrams (particle-particle scattering and hole-hole scattering) and

$$\mathcal{T}^{(2)}_{1,\rm bub}(p,\omega) = \int\frac{d^3q}{(2\pi)^3}|V_1(q)|^2\frac{f^1_{\mathbf{p}-\mathbf{q}}}{\omega-(\mathbf{p}-\mathbf{q})^2/(2m)} \tag{25}$$

is the contribution from particle-hole scattering. This calculation leads to two important conclusions. First, the presence of the degenerate 1-fermions affects scattering in the particle-particle and hole-hole channel and also scattering in the particle-hole channel, but the effects of occupancy of intermediate states cancel in the total, which to second order is given in terms of the T-matrix *in vacuo*. Second, even though the self-energy may be written in the form

$$\Sigma_1 = \mathrm{Tr}\mathcal{T}_1 G_3^0, \tag{26}$$

with the T matrix calculated to second order in the ladder approximation, it leads to an expression of the form (5) where the T matrix contains both ladder and bubble contributions. Only for nondegenerate 1-fermions are the bubble diagrams unimportant compared with the ladder diagrams because $f^1 \ll 1$. By extending the above arguments to higher-order terms, one sees that the self-energy calculated from Eq. (26) with $\mathcal{T}_1$ calculated in the ladder approximation agrees with Eq. (5) only for nondegenerate 1-fermions.

B. Arbitrary order

In higher-order processes, a qualitatively new feature appears: to obtain the result (5), with the T-matrix given by Eq. (6), one cannot use Eq. (26) with the T-matrix calculated in the ladder approximation. To obtain the correct result for $m/m_3 \to 0$, the nth order contribution to the self-energy has the form

$$\Sigma_1^{(n)}(\tau_b-\tau_a) = -(-V_1)^n\int_0^\beta d\tau_1\cdots d\tau_{n-2}G_1(\tau_b-\tau_{n-2}) \times G_1(\tau_{n-2}-\tau_{n-3})\cdots G_1(\tau_1-\tau_a)[G_3(\tau_b-\tau_{n-2}) \times G_3(\tau_{n-2}-\tau_{n-3})\cdots G_3(\tau_1-\tau_a)G_3(\tau_a-\tau_b) + \text{all } \tau \text{ permutations}]. \tag{27}$$

The momentum sums are suppressed for the moment to highlight the essential parts of the reasoning. We refer to this term as an nth-order contribution, even though we use renormalized propagators, which may give rise to contributions of higher order in V_1 when expressed in terms of bare propagators. The first term in the square brackets corresponds to Eq. (26) with $\mathcal{T}$ calculated is the ladder approximation, and it does not give the result (5) for the self-energy in the limit $m_3/m \gg 1$. However, if one adds to it contributions corresponding to all possible ways of attaching the interactions occurring at times $\tau_1 \ldots \tau_{n-2}$ to the 3-bubble with vertices at τ_a and τ_b, one does indeed recover the result (5). This procedure is indicated by the last line of (27) and yields in third order the two diagrams depicted in Fig. 4(b). The structure of a typical high-order diagram generated in this way is illustrated in Fig. 4(c). To show that (27) produces the correct impurity result, we use the fact that the noninteracting 3-propagator for $m/m_3 \to 0$ becomes

$$G_3^0(p,\tau) = \begin{cases} f_p^3 e^{-(\epsilon_3-\mu_3)\tau} & \text{for } \tau < 0 \\ -e^{-(\epsilon_3-\mu_3)\tau} & \text{for } \tau > 0, \end{cases} \tag{28}$$

where $\tau < 0$ corresponds to the propagation of a 3-hole and $\tau > 0$ to the propagation of a 3-particle. Self-energy contributions to G_3 can be absorbed in the chemical potential μ_3 for low T and $m/m_3 \ll 1$. The point is that for any value of $\tau_a, \tau_b, \tau_1, \ldots, \tau_{n-2}$ between 0 and β, only one term inside the square brackets in (27) will have one hole propagator and $n-1$ propagators for the 3-particles. This term will scale as $\sim f_q^3$. All other terms have at least two hole propagators and will be suppressed in the limit of low concentration of the 3-particles. Note that the ladder diagram is not enough to obtain the leading order diagram in f^3 for any value of $\tau_a, \tau_b, \tau_1, \ldots, \tau_{n-2}$: one has to include diagrams corresponding to all possible ways of attaching $\tau_1, \ldots, \tau_{n-2}$ to the 3-bubble. In the limit $m/m_3 \to 0$, the momentum integrals in (27) decouple and the integral over the 3-hole line yields the density n_3. We obtain

$$\Sigma_1^{(n)}(\tau_b - \tau_a) = n_3 V_1^n \int_0^\beta d\tau_2 \ldots d\tau_{n-1} G_1(\tau_b - \tau_{n-2}) \times G_1(\tau_{n-2} - \tau_{n-3}), \ldots, G_1(\tau_1 - \tau_a). \tag{29}$$

In frequency space this reads

$$\Sigma_1^{(n)}(\omega) = n_3 V_1 \left[V_1 G_1(\omega)\right]^{n-1}. \tag{30}$$

Summing all orders for Σ gives

$$\Sigma_1(\omega) = n_3[1 - V_1 G_1(\omega)]^{-1} V_1 = n_3 \mathcal{T}_1(\omega). \tag{31}$$

This agrees with (5) and we have shown that one recovers the correct impurity result for the self-energy in the limit of n_3 small and $m/m_3 \to 0$, when all crossed diagrams of the type illustrated in Fig. 4(c) are included.

The same argument applies to vertex corrections. Consider 1- and 2-fermions simultaneously scattering on a 3-particle. A typical diagram needed to be included to recover the correct impurity result is shown in Fig. 4(d): For an nth order diagram, one has to include all possible ways of attaching the interactions occurring at $\tau_1, \ldots, \tau_n$ to the n propagators in the 3-loop. In this way, the term where there is only one hole in the 3-loop is included for any value of the time arguments. This term scales as n_3 whereas all other diagrams are suppressed by higher powers of n_3. When these diagrams are included to all orders, the effective interaction between a 1-fermion and a 2-fermion both scattering on a 3-atom becomes

$$\begin{aligned} V_{\text{eff}} &= n_3[1 - V_2 G_2(\omega_2)]^{-1} V_2 [1 - V_1 G_1(\omega_1)]^{-1} V_1 \\ &= n_3 \mathcal{T}_1(\omega_1) \mathcal{T}_2(\omega_2). \end{aligned} \tag{32}$$

This agrees with the impurity scattering result given by (7).

C. Higher loops and the x-ray edge problem

So far we have considered diagrams in which there is a single fermion loop containing fermions in states 1 and 2. We now comment on the effect of including contributions with a higher number of loops. The problem under consideration in this paper has a number of points in common with the x-ray edge problem, where the contributions from terms containing many fermion loops change qualitatively the nature of the threshold behavior [21,22] from a step function at the Fermi surface when a single fermion loop is included to a power law whose exponent depends on the phase shift for scattering of an electron in the conduction band from a deep hole. In the x-ray edge problem, conduction electrons scatter from a deep hole, which is present only for times between that at which the electron–deep-hole pair is created and that at which it is destroyed. The complications in the x-ray edge problem are due to the fact that the higher-order loop contributions depend on the times at which the particle-hole pair is created and destroyed. In the problem under consideration in this paper, however, the heavy atoms in the state 3 are present for all time. The effect of the higher-order loops is simply to renormalize the propagator for a 3-atom. The self-energy of a 3-atom depends on energy but, within the approximation of a short-range potential made above, is independent of momentum. When higher loop contributions are included, the chemical potential of the impurities must be adjusted so that the number of impurities is equal to the required value.

D. Analogy with "shadowing" in nuclear physics

The result (15) has a simple interpretation, since it is equivalent to the statement that the self-energy of a particle-hole pair due to interaction with an impurity is proportional to $e^{2i(\delta_2-\delta_1)} - 1$. Since the self-energy is proportional to the T matrix for scattering of a pair from an impurity, which is in turn proportional to $S-1$, where S is the corresponding S matrix, this implies that $S = e^{2i(\delta_2-\delta_1)}$. In physical terms, this says that the extra phase acquired by the pair is the sum of the phase changes experienced by a particle in state 2 and a hole in state 1. The reason that vertex corrections, which correspond to interference terms, are so important in the present problem is that the external field creates a particle and the hole at the same point in space. Thus, if, say, the particle is close to an impurity,

the hole will also be close to an impurity. If only self-energy corrections are included, this is equivalent to assuming that the particle and the hole are uncorrelated in space.

Insight into the result for the line shift may be obtained by making use of the identity

$$\sin 2(\delta_1 - \delta_2) = \sin 2\delta_1(1 - 2\sin^2\delta_2) - \sin 2\delta_2(1 - 2\sin^2\delta_1), \tag{33}$$

which implies that the energy shift is given by the real parts of the self-energy of a 1-fermion and a 2-hole, multiplied by factors $1 - 2\sin^2\delta$. To interpret this result, we observe that the total cross section for scattering of a 3-atom by a σ-fermion is proportional to $\sin^2\delta_\sigma/k^2$, where k is the wave number of the atom. If one changes ones perspective and regards the process as the interaction of an impurity fermion with a particle-hole pair, this equation implies that the amplitude of an impurity fermion at the position of the 2-hole is reduced by an amount $\sim\sin^2\delta_1$ due to scattering from the 1-fermion, and likewise for the amplitude of the impurity at the 2-hole. This is reminiscent of the experimental observation that the total cross section for scattering of pions from deuterons is less than the sum of the cross sections for scattering of a pion from a single neutron and a single proton, a phenomena referred to as "shadowing." It reflects the fact that the neutron and proton in the deuteron are correlated, and therefore the pion field incident on, e.g., the proton is reduced by scattering from the neutron [18]. The analogy between the two situations is not complete, however, since in the problem considered by Glauber the wavelength of the pion is small compared with the separation of the neutron and proton in the deuteron, while in the problem under investigation here the wavelength of the particle and the hole is large compared with their separation, which is initially zero. As a consequence, where k^2 appears in the present problem, this is replaced by a factor $\propto\langle 1/r^2\rangle$, the average of the inverse square of the separation of the neutron and proton in the deuteron.

V. CONCLUDING REMARKS

In this article we have solved a simple model for clock shifts for hyperfine transitions between states of a fermionic atom in the presence of a low density of much more massive atoms. The calculation shows the importance of vertex corrections, which completely change the dependence of the shift and the width of the clock transition on the scattering phase shifts. The calculations are valid for bystander atoms, either fermionic or bosonic, which are much more massive than the majority fermions, and an important problem for the future is to study a finite mass ratio.

Throughout, we have have neglected the interaction between 1-atoms and 2-atoms. When there are no bystanders, the transition has no shift and no width, and this result also holds in the presence of bystanders, provided the 1-3 and 2-3 interactions are identical, since in that case the SU(2) invariance still holds. However, when the 1-3 and 2-3 interactions are different, the line shift and width can be affected by the 1-2 interaction, which is an unexplored effect in the cold atomic gas context.

The calculations indicate that experiments on clock shifts in mixtures of atoms with different masses would be useful. Since pairing correlations are suppressed when species have very different concentrations, these would enable one to obtain information about correlations in a state less complicated than a paired superfluid.

An important theoretical result of our calculations is that it is generally not sufficient to include just ladder diagrams, since in the case considered, particle-hole correlations are necessary in order to recover the correct result for a low density of the minority component.

ACKNOWLEDGMENTS

We are grateful to H. T. C. Stoof for seminal discussions at ECT* in Trento (Italy), and GMB and CJP would like to thank ECT* for hospitality. We thank Wolfgang Götze for helpful correspondence.

[1] L. C. Balling, R. J. Hanson, and F. M. Pipkin, Phys. Rev. **133**, A607 (1964); **135**, AB1(E) (1964).
[2] J. M. V. A. Koelman, S. B. Crampton, H. T. C. Stoof, O. J. Luiten, and B. J. Verhaar, Phys. Rev. A **38**, 3535 (1988).
[3] S. Gupta, Z. Hadzibabic, M. W. Zwierlein, C. A. Stan, K. Dieckmann, C. H. Schunck, E. G. M. van Kempen, B. J. Verhaar, and W. Ketterle, Science **300**, 1723 (2003).
[4] M. W. Zwierlein, Z. Hadzibabic, S. Gupta, and W. Ketterle, Phys. Rev. Lett. **91**, 250404 (2003).
[5] C. Chin, M. Bartenstein, A. Altmeyer, S. Riedl, S. Jochim, J. H. Denschlag, and R. Grimm, Science **305**, 1128 (2004).
[6] Y. Shin, C. H. Schunck, A. Schirotzek, and W. Ketterle, Phys. Rev. Lett. **99**, 090403 (2007); C. H. Schunck, Y. Shin, A. Schirotzek, and W. Ketterle, Nature **454**, 739 (2008).
[7] J. Kinnunen, M. Rodriguez, and P. Törmä, Science **305**, 1131 (2004).
[8] Z. Yu and G. Baym, Phys. Rev. A **73**, 063601 (2006).
[9] A. Perali, P. Pieri, and G. C. Strinati, Phys. Rev. Lett. **100**, 010402 (2008).
[10] P. Pieri, A. Perali, and G. C. Strinati, Nature Physics **5**, 736 (2009).
[11] Y. He, C.-C. Chien, Q. Chen, and K. Levin, Phys. Rev. Lett. **102**, 020402 (2009).
[12] G. Baym, C. J. Pethick, Z. Yu, and M. W. Zwierlein, Phys. Rev. Lett. **99**, 190407 (2007).
[13] M. Punk and W. Zwerger, Phys. Rev. Lett. **99**, 170404 (2007).
[14] P. Massignan, G. M. Bruun, and H. T. C. Stoof, Phys. Rev. A **77**, 031601(R) (2008).
[15] P. Massignan, G. M. Bruun, and H. T. C. Stoof, Phys. Rev. A **78**, 031602(R) (2008).
[16] S. Basu and E. J. Mueller, Phys. Rev. Lett. **101**, 060405 (2008).
[17] L. G. Aslamazov and A. I. Larkin, Phys. Lett. A **26**, 238 (1968).

[18] R. J. Glauber, Phys. Rev. **100**, 242 (1955).
[19] A. A. Abrikosov, L. P. Gorkov, and I. Ye. Dzyaloshinskii, *Quantum Field Theoretical Methods in Statistical Physics* (Pergamon, Oxford, 1965), §39.
[20] G. Baym, Phys. Rev. **127**, 1391 (1962).
[21] G. D. Mahan, Phys. Rev. **163**, 612 (1967).
[22] P. Nozières and C. T. De Dominicis, Phys. Rev. **178**, 1097 (1969).